Indian Journal of Pure & Applied Physics
Vol. 55, December 2017, pp. 847-856

Heat and mass transfer over a three-dimensional inclined non-linear stretching sheet with convective boundary conditions

Shalini Jain* & Shweta Bohra

Department of Mathematics & Statistics, Manipal University Jaipur, Jaipur 303 007, India

Received 2 December 2016; accepted 6 May 2017

This investigation has been made to study of heat and mass on three-dimensional boundary layer flow of an incompressible fluid due to inclined non-linear stretching sheet with convective boundary conditions. The effect of thermophoresis and chemical reaction has been taken into account. Numerical solution has been obtained for the set of non-linear coupled ordinary equations which are reduced by using similarity transformations from non-linear partial differential equations. Transforms system of equations has been solved using Runge–Kutta–Fehlberg fourth–fifth order method along with shooting technique. Effects of various parameters on velocity, temperature and concentration profiles have been obtained. These results have been presented through graphs and also our analysis explores the physical quantities of interest through the tables.

Keywords: Inclined non-linear stretching sheet, Convective boundary conditions, Thermophoresis chemical reaction

1 Introduction

The fluid flow over a non-linear stretching sheet is relevant to many engineering and industrial applications in the field of chemical, power and metallurgy engineering. Crane[1] has first investigated two dimensional boundary layer flows over a stretching surface. Later this problem was extended by Carragher and Crane[2]. After this pioneering work many researchers have been receiving attention to the study of the flow field over stretching surface[3-12]. Kumaran and Ramanaih[13] examined fluid flow over a quadratic stretching sheet. Earlier, Vajravelu[14] analyzed fluid flow and heat transfer in a viscous fluid over a non-linear stretching sheet. Further, Cortell[15] has given a numerical solution for two specific cases at constant surface temperature and prescribed surface temperature over a non-linear stretching sheet. Bhargav[16] examined the study of boundary layer flow of an incompressible micro polar fluid flowing over a plane sheet stretched non-linearly. Later Hayat[17] also obtained the solution for micro polar fluid for mixed convection flow. Awang[18] described Adomian decomposition method (ADM) for solving the set of boundary-layer equation over a non-linearly stretching sheet. He also analyzed the influence of chemical reaction and a magnetic field. Similarly, many researchers[19-23] investigated flow problems over a non-linear stretching sheet under various conditions. The boundary layer flow of a nanofluid due to stretching sheet has attracted many researchers. Rama and Bhargava[24] obtained numerical result for steady, laminar boundary layer fluid flow over a non-linear stretching sheet in a nanofluid in the influence of Brownian motion and thermophoresis. Semi-analytical/numerical solutions have been given by Rashidi *et al.*[25] in a nanofluid regime adjacent to a non-linearly porous stretching sheet. Recently, several other researchers[26-28] has investigated nanofluid flow over a two dimensional non-linear Stretching sheet. Further, the study of three-dimensional flow past a non-linearly stretched surface has been done by Khan *et al*.[29,30]. He has given analytically and numerical solutions. He has extended his work for nanofluid. Recently, the study of three-dimensional boundary layer flow of nanofluid has been done by Mahanthesh *et al*.[31]over a nonlinearly stretching sheet by considering the nonlinear radiative effect and convective boundary conditions.

Many researchers have shown interest in fluid flow over inclined two or three-dimensional stretching sheet due to its important application such as gas turbines, extrusion of plastic sheets from a die, MHD power generators, the boundary layer along a liquid film condensation process and polymer industries as well as in the field of aeronautics, chemical engineering and planetary magnetosphere. Shit and Haldar[32] studied the combined effects of thermal radiation and Hall current in laminar boundary-layer flow over an inclined permeable stretching sheet with variable viscosity. The

*Corresponding author (E-mail: shalini.jain@jaipur.manipal.edu)

study of heat and mass transfer including chemical reaction has also been received keen interest by researchers due its applications in engineering and geophysics such as dehydration at the surface of a water body drying, geothermal reservoirs, thermal insulation, drying of porous solids, geothermal pool, enhanced oil recovery, cooling of nuclear reactors, evaporation at the surface of a water body, fibrous insulation, pollution studies, cooling the polymer production and manufacturing of ceramics etc. Shit and Majee[33] discussed combined effect of radiation and chemical reaction in MHD flow over a non-linear stretching sheet. Gireesha and Mahanthesh[34] studied heat and mass transfer of visco elastic fluid in non-uniform channel with chemical reaction and Hall current effect. In recent years, many researchers[35-37] considered effect of chemical reaction in their investigation with different physical configurations. Ali *et al*.[38] obtained result for the effect of MHD on flow and heat transfer past an inclined stretching sheet. Heat and mass transfer analysis of three-dimensional radiative flow of a Maxwell fluid over an inclined stretching surface has been done by Ashraf *et al*.[39] with thermophoresis effects. He has considered convective boundary conditions for study the heat transfer on convective surface.

Up to best of our knowledge, no study for three-dimensional inclined non-linear stretching sheet has been done so far. Therefore, this investigation is aims to study the heat and mass transfer over three-dimensional non-linear stretching sheet with convective boundary conditions.

2 Mathematical Formulation

In present study, three-dimensional steady, laminar boundary layer flow of an incompressible fluid is considered over an inclined non-linearly stretching surface in two directions *x*- and *y*- respectively. Figure 1 presents the schematic diagram of the problem. The surface velocities in *x* and *y* directions are given by; $u_{\mathrm{w}} = a(x+y)^{\mathrm{n}}, v_{\mathrm{w}} = b(x+y)^{\mathrm{n}}$, respectively, where *a, b* and $n > 0$ are constants. T_{w} and T_∞ are temperature at wall/sheet and ambient temperature, respectively, here T_{c} is convective environment temperature which maintain the surface temperature T_{w}. C_{w} and C_∞ are concentration at sheet and ambient concentration, respectively. Heat and mass transfer study is being done with chemical reaction and thermophoretic velocity component along normal to the surface.

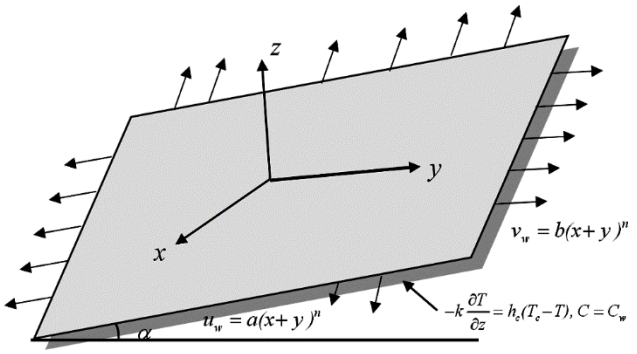

Fig. 1 — Schematic diagram.

The steady three-dimensional boundary layer equations are Ashraf *et al*.[33]

$$\frac{\partial u}{\partial x} + \frac{\partial v}{\partial y} + \frac{\partial w}{\partial z} = 0, \quad \ldots (1)$$

$$\rho\left[u\frac{\partial u}{\partial x} + v\frac{\partial u}{\partial y} + w\frac{\partial u}{\partial z}\right] = \mu\frac{\partial^2 u}{\partial z^2} + \rho g[\beta_{\mathrm{T}}(T - T_\infty) + \beta_{\mathrm{c}}(C - C_\infty)]\cos\alpha - \frac{\mu u}{k_0}, \quad \ldots (2)$$

$$\rho\left[u\frac{\partial v}{\partial x} + v\frac{\partial v}{\partial y} + w\frac{\partial v}{\partial z}\right] = \mu\frac{\partial^2 v}{\partial z^2} + \rho g[\beta_{\mathrm{T}}(T - T_\infty) + \beta_{\mathrm{c}}(C - C_\infty)]\sin\alpha - \frac{\mu v}{k_0}, \quad \ldots (3)$$

$$u\frac{\partial T}{\partial x} + v\frac{\partial T}{\partial y} + w\frac{\partial T}{\partial z} = \frac{\kappa}{\rho C_{\mathrm{P}}}\frac{\partial^2 T}{\partial z^2}, \quad \ldots (4)$$

$$u\frac{\partial C}{\partial x} + v\frac{\partial C}{\partial y} + w\frac{\partial C}{\partial z} = D_{\mathrm{m}}\frac{\partial^2 C}{\partial z^2} - \frac{\partial}{\partial z}[V_{\mathrm{T}}(C - C_\infty)] - k_{\mathrm{r}}(C - C_\infty), \quad \ldots (5)$$

where, *u, v* and *w* are corresponding velocity components in *x*-, *y*- and *z*- directions. *T* and *C* are fluid temperature and concentration, *g* is gravitational acceleration, μ is dynamic viscosity, ρ is density, $\nu = \mu/\rho$ is kinematic viscosity, k_0 is permeability coefficient, β_{T} and β_{c} are thermal and concentration expansion coefficients respectively, κ is thermal conductivity of the fluid, C_{P} is specific heat captaincy

at constant pressure P, D_{m} is mass diffusivity, α is angle of an inclined sheet, k_{r} is rate of chemical reaction and V_{T} is the thermophoretic velocity. The thermophoretic velocity V_{T} is defined as:

$$V_{\mathrm{T}} = \frac{-k\nu}{T_{\mathrm{r}}}\frac{\partial T}{\partial z} \quad \ldots(6)$$

where, k is thermophoretic coefficient and T_{r} is reference temperature.

Under the convective boundary conditions with heat transfer coefficient h_{c} are given as:

at $z = 0, u = u_{\mathrm{w}}, v = v_{\mathrm{w}}, w = 0,$

$$-\kappa\frac{\partial T}{\partial z} = h_{\mathrm{c}}(T_{\mathrm{c}} - T), C = C_{\mathrm{w}}$$

at $z \to \infty, u \to 0, v \to 0, T \to T_{\infty}, C \to C_{\infty}$ $\ldots(7)$

here, we take $h_{\mathrm{c}} = {c^*}/{\sqrt{x^{1-\mathrm{n}}}}$, where c^* is constant.

Introducing similarity transformation, followed by Mahanthesh *et al*.[29] are given as;

$$\eta = \sqrt{\frac{a}{\nu}}\,(x+y)^{\frac{\mathrm{n}-1}{2}}z, u = a(x+y)^{\mathrm{n}}f'(\eta),$$

$$v = a(x+y)^{\mathrm{n}}g'(\eta),$$

$$w = -\sqrt{a\nu}(x+y)^{\frac{\mathrm{n}-1}{2}}$$

$$\left[\frac{\mathrm{n}+1}{2}\big(f(\eta)+g(\eta)\big) + \frac{\mathrm{n}-1}{2}\eta\big(f'(\eta)+g'(\eta)\big)\right],$$

$$T - T_{\infty} = (T_{\mathrm{c}} - T_{\infty})\,\theta(\eta),$$

$$C - C_{\infty} = (C_{\mathrm{w}} - C_{\infty})\,\phi(\eta) \quad \ldots(8)$$

where, f, g and θ are non-dimensional functions of η. Using Eqs (6) and (8) in Eqs (1)-(5) under the boundary conditions Eq. (7), the continuity Eq. (1) is identically satisfied and we get the reduced form of Eqs (2)-(5) in non-dimensional form with respect to boundary condition Eq. (6) as:

$$f''' + \frac{n+1}{2}(f+g)f'' - n(f'+g')f' - \frac{f'}{K} + \delta(\theta + N_{\mathrm{b}}\phi)\cos\alpha = 0, \quad \ldots(9)$$

$$g''' + \frac{n+1}{2}(f+g)g'' - n(f'+g')g' - \frac{g'}{K} + \delta(\theta + N_{\mathrm{b}}\phi)\sin\alpha = 0, \quad \ldots(10)$$

$$\theta'' + Pr\left(\frac{n+1}{2}\right)(f+g)\theta' = 0, \quad \ldots(11)$$

$$\phi'' + Sc\left(\frac{n+1}{2}\right)(f+g)\phi' - Sc\tau(\phi\theta'' + \theta'\phi') - ScKr\phi = 0, \quad \ldots(12)$$

Subjected to boundary conditions:

at $\eta = 0, f' = 1, g' = c, f = 0, g = 0, \theta' = Bi(\theta - 1), \phi = 1$

as $\eta \to \infty, f' \to 0, g' \to 0, \theta \to 0, \phi \to 0,$ $\ldots(13)$

where, the primes denote the differentiation with respect to η, the dimensionless radial coordinate.

$Pr = \frac{\mu C_{\mathrm{P}}}{\kappa}$, is Prandtl number, physical nature of Pr represents the comparison between momentum and thermal diffusion. Pr is taken to be 0.71 and 7.0 which corresponds to air and water, respectively.

$Sc = \frac{\nu}{D^{\mathrm{m}}}$, is Schmidt number. Sc represents the ratio of the momentum to the mass diffusivity. For $Sc <$ 1species diffusion rate exceeds the momentum diffusion rate and vice versa for $Sc > 1$. For $Sc = 1$ both diffusion rates are the same and the momentum and concentration boundary layer thickness equal in the regime. The value of Schmidt number is taken as (Sc = 0.22, 0.66, 0.94, 1, 2, 2.62) representing diffusing chemical species of most common interest in air for hydrogen, oxygen, carbon dioxide, methanol, ethyl benzene and propyl benzene, respectively. $N_{\mathrm{b}} = \frac{\beta_{\mathrm{c}}(C_{\mathrm{w}} - C_{\infty})}{\beta_{\mathrm{T}}(T_{\mathrm{c}} - T_{\infty})}$, is concentration to thermal buoyancy ratio parameter. $N_{\mathrm{b}} = 1$ shows that the thermal and species buoyancy force are of the same order of magnitude and assist each other. When $N_{\mathrm{b}} < 1$, thermal buoyancy will dominate concentration buoyancy effects and vice versa for $N_{\mathrm{b}} > 1$.

$\delta = \frac{Gr_{\mathrm{x}}}{Re_{\mathrm{x}}^2}$ is local buoyancy parameter ratio.

Where:

$Gr_{\mathrm{x}} = \frac{g\beta_{\mathrm{T}}(T_{\mathrm{c}} - T_{\infty})(x+y)^3}{\nu^2}$ and

$Re_{\mathrm{x}} = \frac{u_{\mathrm{w}}(x+y)}{\nu}$ are local Grashof number and Reynolds number, respectively,

$K = \frac{k_0 u_{\mathrm{w}}}{\nu(x+y)}$ is local permeability parameter,

$\tau = \frac{-k(T_{\mathrm{c}} - T_{\infty})}{T_{\mathrm{r}}}$ is thermophoretic parameter and

$Kr = \frac{k_r(x+y)}{u_{\mathrm{w}}}$ is local chemical reaction parameter.

By considering the interest of practical and engineering primary; we can describe the physical quantities such

as local skin friction coefficients, local Nusselt number and local Sherwood number:

$$C_{\mathrm{fx}}=\frac{\tau_{\mathrm{zx}}}{\rho u_{\mathrm{w}}^2}, C_{\mathrm{fy}}=\frac{\tau_{\mathrm{zy}}}{\rho v_{\mathrm{w}}^2}, Nu=\frac{(x+y)q_{\mathrm{w}}}{\kappa(T_{\mathrm{c}}-T_{\infty})},$$
$$Sh=\frac{(x+y)m_{\mathrm{w}}}{D_{\mathrm{m}}(C_{\mathrm{w}}-C_{\infty})}, \quad \ldots(14)$$

where, the shear stresses correspondingly in *x, y* directions τ_{zx} and τ_{zy}, heat flux q_{w} and mass flux m_{w} is the at the wall are defined as:

$$\tau_{\mathrm{zx}}=\mu\left(\frac{\partial u}{\partial z}+\frac{\partial w}{\partial x}\right)_{\mathrm{z=0}}, \tau_{\mathrm{zy}}=\mu\left(\frac{\partial v}{\partial z}+\frac{\partial w}{\partial y}\right)_{\mathrm{z=0}},$$

$$q_{\mathrm{w}}=-\kappa\left(\frac{\partial T}{\partial z}\right)_{\mathrm{z=0}}, m_{\mathrm{w}}=-D_{\mathrm{m}}\left(\frac{\partial C}{\partial z}\right)_{\mathrm{z=0}} \quad \ldots(15)$$

By using similarity transformation and Eq. (15) in Eq. (14), we get:

$$Re_{\mathrm{x}}^{1/2}C_{\mathrm{fx}}=f''(0),$$
$$c^{3/2}Re_{\mathrm{y}}^{1/2}C_{\mathrm{fy}}=g''(0),$$
$$Re_{\mathrm{x}}^{-1/2}Nu_{\mathrm{x}}=-\theta'(0), Re_{\mathrm{x}}^{-1/2}Sh_{\mathrm{x}}=-\phi'(0) \quad \ldots(16)$$

where, $Re_{\mathrm{y}}=\frac{u_{\mathrm{w}}(x+y)}{\nu}$ and $Re_{\mathrm{x}}=\frac{v_{\mathrm{w}}(x+y)}{\nu}$ are the local Reynolds number along *x*-and *y*- direction, respectively. The vertical component of velocity at far field condition can be defined as:

$$w(x,y,\infty)=-\sqrt{a\nu}(x+y)^{\frac{n-1}{2}}\left[\frac{n+1}{2}\left(f(\infty)+g(\infty)\right)\right].$$

3 Method of Solution

In present problem, shooting method with fourth-fifth order Runge–Kutta-Fehlberg integration procedure has been applied for solving the set of nonlinear ordinary differential Eqs (9) to (12) under the boundary conditions Eq. (13). Runge–Kutta–Fehlberg method (or Fehlberg method) is an algorithm in numerical analysis for the numerical solution of ordinary differential equations and is a method of order 4 with an error estimator of order 5, the algorithm is as follow:

Step 1: Convert the boundary value problem into initial value problem.

Step 2: Choose the suitable finite value of η_{∞}.

Step 3: Shooting technique is used to guess missing initial conditions by an iterative process until boundary conditions are satisfied.

Step 4: Solve the reduced system of the initial value equations by Runge-Kutta-Fehlberg method by taking step size $h = 0.001$.

Step 5: This process was repeated until we obtained results correct up to the desired accuracy of 10^{-6} level.

The formula of RKF-45 is followed by:

Each step requires the use of the following six values:

$$k_1=hf(x_{\mathrm{k}},y_{\mathrm{k}})$$

$$k_2=hf\left(x_{\mathrm{k}}+\frac{1}{4}h,y_{\mathrm{k}}+\frac{1}{4}k_1\right)$$

$$k_3=hf\left(x_{\mathrm{k}}+\frac{3}{8}h,y_{\mathrm{k}}+\frac{3}{32}k_1+\frac{9}{32}k_2\right)$$

$$k_4=hf\left(x_{\mathrm{k}}+\frac{12}{13}h,y_{\mathrm{k}}+\frac{1932}{2197}k_1-\frac{7200}{2197}k_2+\frac{7296}{2197}k_3\right)$$

$$k_5=hf\left(x_{\mathrm{k}}+h,y_{\mathrm{k}}+\frac{439}{216}k_1-8k_2+\frac{3680}{513}k_3-\frac{845}{4104}k_4\right)$$

$$k_6=hf\begin{pmatrix}x_{\mathrm{k}}+\frac{h}{2},y_{\mathrm{k}}-\frac{8}{27}k_1\\+2k_2-\frac{3544}{2565}k_3+\frac{1859}{4104}k_4-\frac{11}{40}k_5\end{pmatrix}$$

Using above constants and applying RKF-45 method, we obtain approximation solution of I.V.P.:

$$y_{\mathrm{k+1}}=y_{\mathrm{k}}+\frac{25}{216}k_1+\frac{1408}{2565}k_3+\frac{2197}{4104}k_4-\frac{1}{5}k_5$$

For improved the above solution, using RKF-45 method, we obtain:

$$y_{\mathrm{k+1}}=y_{\mathrm{k}}+\frac{16}{135}k_1+\frac{6656}{12825}k_3+\frac{28561}{56430}k_4$$
$$-\frac{9}{50}k_5+\frac{2}{55}k_6.$$

4 Validation of Present Study

Table 1 shows a comparison of numerical values of $f''(0)$ and $g''(0)$ obtained in the present investigation in the absence of permeability *K* and local buoyancy parameter δ with the results obtained by Khan *et al*.[30] and Mahanthesh *et al*.[31]. It is noted that the results obtained are in excellent agreement with literature available.

Table 2 and Table 3 show the comparison between the result obtained using bvp4c solver in MATLAB

and Runge-Kutta-Fehlberg fourth-fifth method with shooting technique. It is observed that results obtained from both the methods are well in agreement. Also noted that order of convergence of result obtained from Runge-Kutta-Fehlberg fourth-fifth method with shooting technique is more than of bvp4c solver in MATLAB.

Table 1 — Comparison between the results of present study with the results reported by Khan *et al.*[30] and Mahanthesh *et al.*[31] for $f''(0)$ and $g''(0)$ for $K = \delta = 0$.

n	Stretching parameter c	Literature[30]		Literature[31]		Present study	
		$f''(0)$	$g''(0)$	$f''(0)$	$g''(0)$	$f''(0)$	$g''(0)$
1	0	-1	0	-1	0	-1	0
1	0.5	-1.224745	-0.612372	-1.22474	-0.61237	-1.22474	-0.61237
1	1	-1.414214	-1.414214	-1.41421	-1.41421	-1.41421	-1.41421
3	0	-1.624356	0	-1.62436	0	-1.62436	0
3	0.5	-1.989422	-0.994711	-1.98942	-0.99471	-1.98942	-0.99471
3	1	-2.297186	-2.297186	-2.29719	-2.29712	-2.29719	-2.29712

Table 2 — Variation of $f''(0)$ and $g''(0)$ for different values of K, Kr, δ, τ, Bi and N_b when $Pr = 2$, $Sc = 1$, $c = 0.5$, $\alpha = \pi/4$.

n	K	N_b	δ	Kr	τ	Bi	$f''(0)$		$g''(0)$	
							Runge-Kutta Fehlberg 4-5order method with shooting technique	*bvp4c*	Runge-Kutta Fehlberg 4-5order method with shooting technique	*bvp4c*
	0.5	0.2	0.2	0.5	0.2	0.3	-1.850990	-1.850882	-0.914142	-0.914130
	1						-1.561881	-1.560715	-0.768762	-0.768765
	10						-1.251390	-1.244871	-0.612141	-0.609177
		0.2					-1.850990	-1.850882	-0.914142	-0.914130
		0.5					-1.836821	-1.836843	-0.899300	-0.899132
		1					-1.813426	-1.813560	-0.874500	-0.874271
			0.2				-1.850990	-1.850882	-0.914142	-0.914130
			0.5				-1.821437	-1.821434	-0.882617	-0.882734
			1				-1.773621	-1.773474	-0.831664	-0.831660
1				0.5			-1.850990	-1.850882	-0.914142	-0.914130
				1			-1.851795	-1.851664	-0.915013	-0.915004
				2			-1.852735	-1.852614	-0.916062	-0.916058
					0.2		-1.850990	-1.850882	-0.914142	-0.914130
					0.3		-1.851093	-1.850931	-0.914220	-0.914185
					0.5		-1.851275	-1.851029	-0.914417	-0.914294
						0.3	-1.850990	-1.850882	-0.914142	-0.914130
						1	-1.839250	-1.839249	-0.901800	-0.901763
						5	-1.824809	-1.824808	-0.886400	-0.886408
	0.5	0.2	0.2	0.5	0.2	0.3	-2.161687	-2.161686	-1.071780	-1.071775
	1						-1.917317	-1.917316	-0.948900	-0.949055
	10						-1.666700	-1.666792	-0.823141	-0.823140
		0.2					-2.161687	-2.161686	-1.071780	-1.071775
		0.5					-2.149690	-2.149688	-1.058556	-1.058554
		1					-2.129800	-2.129794	-1.036660	-1.036655
			0.2				-2.161687	-2.161686	-1.071780	-1.071775
			0.5				-2.139183	-2.139182	-1.047097	-1.047096
			1				-2.102300	-2.102283	-1.006691	-1.006696
2				0.5			-2.161687	-2.161686	-1.071780	-1.071775
				1			-2.162284	-2.162248	-1.072435	-1.072440
				2			-2.162970	-2.162967	-1.073278	-1.073283
					0.2		-2.161687	-2.161686	-1.071780	-1.071775
					0.3		-2.161730	-2.161725	-1.071822	-1.071821
					0.5		-2.161810	-2.161804	-1.071916	-1.071913
						0.3	-2.161687	-2.161686	-1.071780	-1.071775
						1	-2.152669	-2.152668	-1.061931	-1.061940
						5	-2.140000	-2.139999	-1.048140	-1.048132

Table 3 – Variation of $-\theta'(0)$and $-\phi'(0)$ for different values of *K, Kr*, δ, τ, *Bi* and N_b when *Pr* = 2, *Sc* = 1, *c* = 0.5, α = $\pi/4$.

n	*K*	N_b	δ	*Kr*	τ	*Bi*	$-\theta'(0)$		$-\phi'(0)$	
							Runge-Kutta Fehlberg 4-5 method with shooting technique	*bvp4c*	Runge-Kutta Fehlberg 4-5 method with shooting technique	*bvp4c*
	0.5	0.2	0.2	0.5	0.2	0.3	0.230075	0.230062	0.996728	0.997069
	1						0.233167	0.233145	1.021513	1.021783
	10						0.236310	0.236305	1.052721	1.052820
		0.2					0.230075	0.230062	0.996728	0.997069
		0.5					0.230328	0.230330	0.998511	0.999030
		1					0.230761	0.230759	1.002212	1.002244
			0.2				0.230075	0.230062	0.996728	0.997069
			0.5				0.230595	0.230590	1.000905	1.000971
1			1				0.231397	0.231392	1.007126	1.007154
				0.5			0.230075	0.230062	0.996728	0.997069
				1			0.230041	0.230030	1.240381	1.240386
				2			0.229998	0.229996	1.610518	1.610511
					0.2		0.230075	0.230062	0.996728	0.997069
					0.3		0.230065	0.230060	1.013358	1.013361
					0.5		0.230061	0.230056	1.045725	1.046129
						0.3	0.230075	0.230062	0.996728	0.997069
						1	0.497635	0.497654	1.036541	1.036570
						5	0.829717	0.830011	1.085600	1.086036
	0.5	0.2	0.2	0.5	0.2	0.3	0.241463	0.241462	1.107164	1.107163
	1						0.243365	0.243363	1.133235	1.133232
	10						0.245232	0.245229	1.162885	1.162882
		0.2					0.241463	0.241462	1.107164	1.107163
		0.5					0.241635	0.241630	1.109371	1.109367
		1					0.241910	0.241902	1.112823	1.112971
			0.2				0.241463	0.241462	1.107164	1.107163
			0.5				0.241761	0.241754	1.110971	1.110972
2			1				0.242212	0.242210	1.117068	1.117066
				0.5			0.241463	0.241462	1.107164	1.107163
				1			0.241447	0.241445	1.333388	1.333386
				2			0.241428	0.241425	1.686845	1.686843
					0.2		0.241463	0.241462	1.107164	1.107163
					0.3		0.241471	0.241461	1.124830	1.124828
					0.5		0.241461	0.241458	1.160319	1.160317
						0.3	0.241463	0.241462	1.107164	1.107163
						1	0.553632	0.553628	1.154336	1.154335
						5	0.996282	0.996281	1.221761	1.221757

5 Results and Discussion

In the present study we obtained numerical solution for heat and mass transfer of an incompressible fluid flow over an inclined non-linear stretching sheet. Results obtained for axial and transverse velocity profile, temperature and concentration profile for various pertinent parameters are depicted through Figs 2-9. Numerical values of physical quantities of interest are presented in Tables 2 and 3.

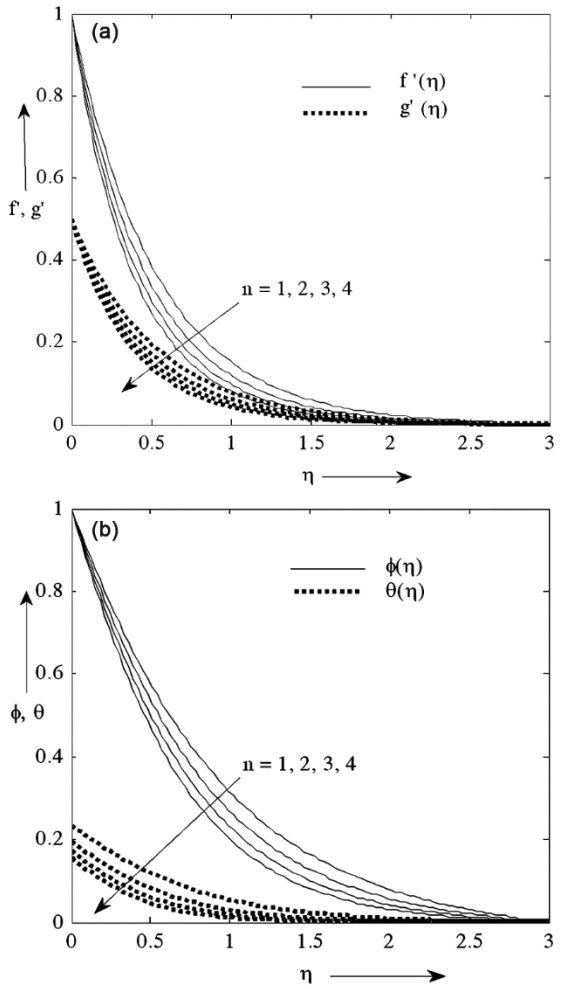

Fig. 2 — Effect of variation of the power law index on (a) axial and transverse velocity (b) temperature and concentration profiles when $N_b = \delta = \tau = 0.2$, $\alpha = \pi/4$, $K = 0.5$, $Pr = 0.71$, $Sc = 1$, $Kr = 0.5$, $Bi = 0.3$ and $c = 0.5$.

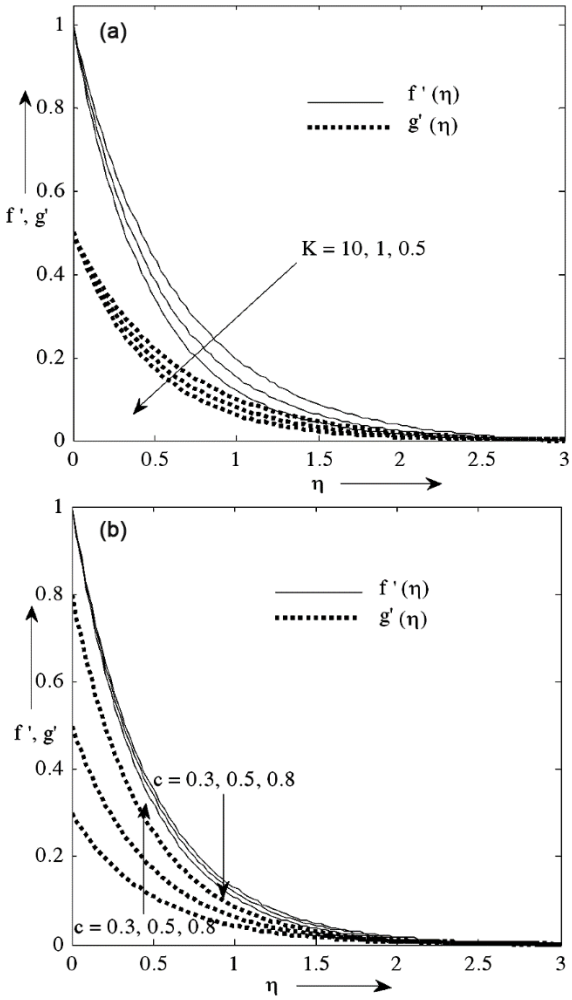

Fig. 3 — Effect of variation of the (a) permeability parameter (b) ratio of stretching rate on the axial and transverse velocity profiles when $N_b = \delta = \tau = 0.2$, $\alpha = \pi/4$, $Pr = 0.71$, $Sc = 1$, $Kr = 0.5$, $Bi = 0.3$ and $n = 2$.

The influence of power law index n on axial velocity $f'(\eta)$ and transverse velocity $g'(\eta)$ temperature distribution $\theta(\eta)$ and concentration distribution $\phi(\eta)$ is plotted in Fig. 2(a,b). It has been observed that the velocity profile, temperature and concentration profile fall down, when n increases. It shows that an increment in non-linearity of the stretching sheet causes decrement in velocity, temperature and concentration profiles.

Figure 3(a) depicts the influence of permeability parameter K. It is noted that both axial and transverse velocity increases with increasing value of K. Because, as permeability increases, Darcy's resistance force reduces, hence the velocity of fluid enhances in both directions. Variation of ratio of stretching rate ($c = b/a$) in axial and transverse velocity is plotted in Fig. 3(b), transverse velocity is directly proportional to stretching rate and inversely proportional to axial velocity. Therefore, it is concluded that when c increases, the flow accelerates downwards causes transverse velocity increases while axial velocity reduces.

Figure 4(a,b) show the influence of K and c on temperature and concentration profile, respectively. The increasing effect of c reduces both temperature and concentration as shown in Fig. 4(a,b). This is due to the reason that as stretching of sheet increases, the intensity of the cooler fluid from the ambient to hotter fluid near the surface enhances. Thus temperature and concentration falls down. Also we observed that thermal and solute boundary layer thickness decreases as K increases. It is due to the reason that as K increases Darcy's resistance force reduces.

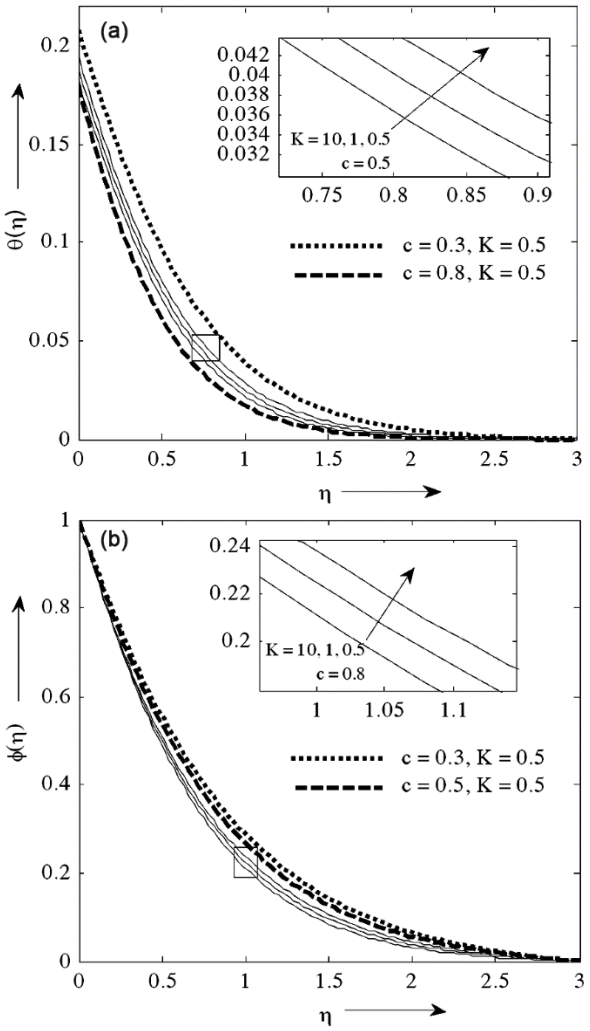

Fig. 4 — Effect of variation of the permeability parameter and stretching ratio on (a) temperature (b) concentration profiles when $N_b = \delta = \tau = 0.2$, $\alpha = \pi/4$, $Pr = 0.71$, $Sc = 1$, $Kr = 0.5$, $Bi = 0.3$ and $n = 2$.

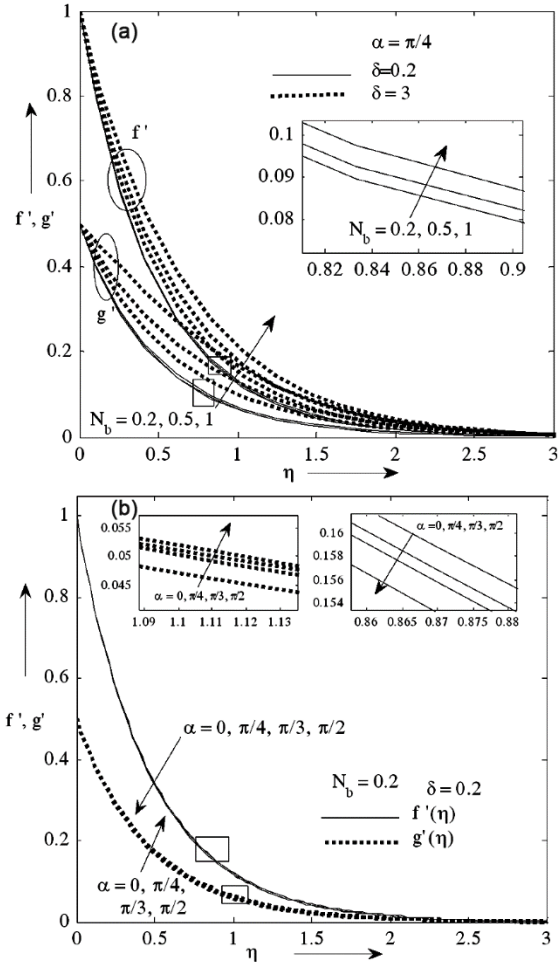

Fig. 5 — Effect of variation of the (a) buoyancy ratio parameter and local buoyancy parameter (b) inclined angle on the axial and transverse velocity profiles when $\tau = 0.2$, $n = 2$, $K = 0.5$, $Pr = 0.71$, $Sc = 1$, $Kr = 0.5$, $Bi = 0.3$ and $c = 0.5$.

The influence of buoyancy ratio parameter N_b, local buoyancy parameter ratio δ and effect of inclined angle α on axial and transverse velocity profile is depicted in Fig. 5(a) and Fig. 5(b), respectively. It is observed that both axial and transverse velocity increases when N_b and δ increases. Because natural convection arises by increasing effect of N_b and δ, which accelerates the flow, hence flow of fluid increases. We observed that velocity along the x-direction reduces while velocity along to y-direction enhances as α increases.

From Fig. 6(a,b) we noticed that temperature and thermal boundary layer thickness and concentration and solute boundary layer thickness decreases when N_b and δ increases. It is noticed that at low value of δ, effect of N_b is dominant comparatively higher value of δ.

Figure 7 shows that concentration profile reduces when value of both, chemical reaction parameter Kr and Schmidt number Sc increases. Sc represents the ratio of momentum to mass diffusivity, so mass diffusion reduces with increasing Sc, which is responsible for falls down in solute boundary layer thickness. The influence of Biot number Bi and thermometric parameter τ on temperature and concentration distribution is plotted in Fig. 8. Increasing effect of Bi number boosts the temperature while increasing value of τ reduces the concentration of the fluid.

Figure 9(a,b) shows the effect of Prandtl number Pr on axial and transverse velocity, temperature and concentration profiles. It has been observed that increasing Pr value reduces the flow and temperature while reverse effect has been seen on concentration profile

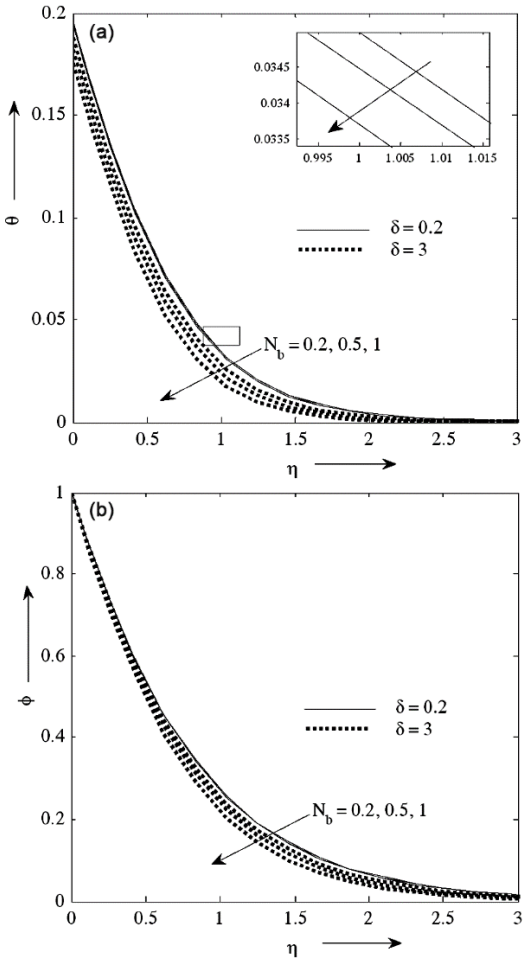

Fig. 6 — Effect of variation of buoyancy ratio parameter and local buoyancy parameter on (a) temperature (b) concentration profiles when $\tau = 0.2$, $\alpha = \pi/4$, $n = 2$, $K = 0.5$, $Pr = 0.71$, $Sc = 1$, $Kr = 0.5$, $Bi = 0.3$ and $c = 0.5$.

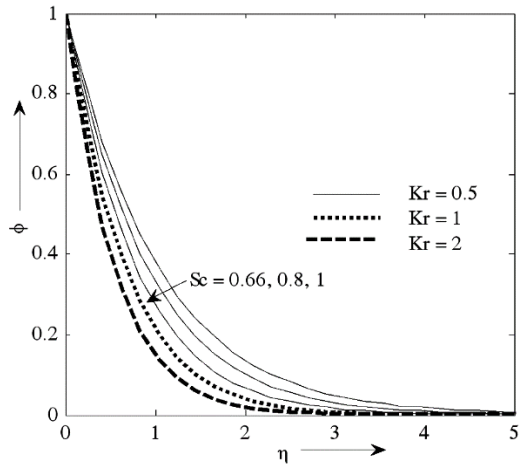

Fig. 7 — Effect of chemical reaction parameter and Schmidt number on concentration distribution when $N_b = \delta = \tau = 0.2$, $\alpha = \pi/4$, $K = 0.5$, $Pr = 0.71$, $n = 2$, $Bi = 0.3$ and $c = 0.5$

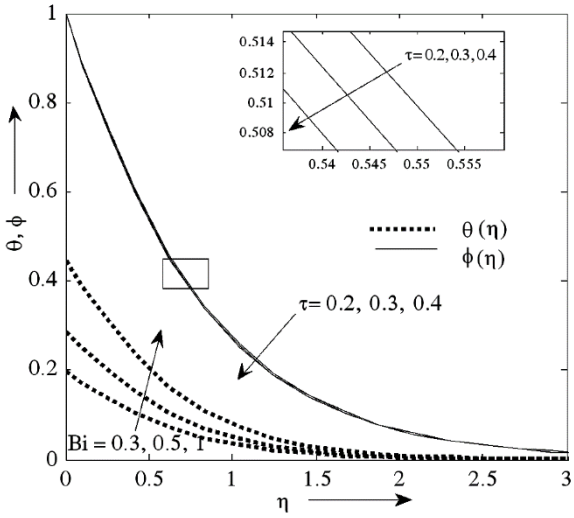

Fig. 8 — Effect of Biot number and thermophoretic parameter on temperature and concentration profiles when $N_b = \delta = 0.2$, $\alpha = \pi/4$, $K = 0.5$, $n = 2$, $Kr = 0.5$, $Sc = 1$, $Pr = 0.71$ and $c = 0.5$.

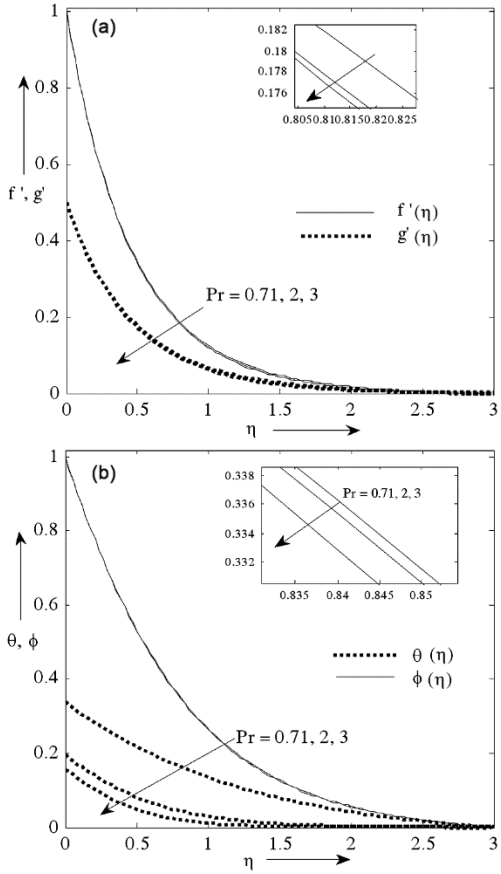

Fig. 9 — Effect of variation in Prandtl number on the (a) axial and transverse velocity (b) temperature and concentration profiles when $N_b = \delta = \tau = 0.2$, $\alpha = \pi/4$, $K = 0.5$, $Sc = 1$, $Kr = 0.5$, $Bi = 0.3$, $n = 2$ and $c = 0.5$.

6 Conclusions

The effect of thermophoretic velocity and chemical reaction parameter on fluid flow, heat and mass transfer over an inclined, non-linearly stretched in two directions, has been analyzed under convective boundary conditions. The numerical solution has been obtained and discussed for the system of formulated problem. It is observed that:

(i) The increasing value of power law index n shows decreasing effect on velocity, temperature and concentration profile.

(ii) The axial velocity, temperature distribution and concentration distribution decrease when stretching ratio parameter c increases while reverse effect has been obtained in case of transverse velocity.

(iii) The concentration boundary layer thickness reduces with the increasing effect of chemical reaction parameter and thermophoretic parameter.

(iv) The thermal boundary layer thickness or temperature increases with the increase of Biot number.

References

1 Crane L J, *Z Angew Math Phys*, 21 (1970) 645.
2 Carragher P & Crane L J, *Z Angew Math Mech*, 62 (1982) 564.
3 Gupta P S & Gupta A S, *Can J Chem Eng*, 55 (1977) 744.
4 Pavlov K B, *Magnitnaya Gidrodinamika*, 4 (1974) 146.
5 Grubka, L G & Bobba K M, *J Heat Transfer*, 107 (1985) 248.
6 Andersson H I, Bech K H & Dandapat B S, *Int J Non-Linear Mech*, 27 (1992) 929.
7 Shit G C, *Int J Appl Math Mech*, 5 (2009) 22.
8 Prasad K V, Dattiand P S & Vajravelu K, *Int J Heat Mass Transfer*, 53 (2010) 879.
9 Chauhan D S & Olkha A, *Chem Eng Commun*, 198 (2011) 1129.
10 Chauhan D S & Rastogi P, *Int J Energy Tech*, 4 (2012) 1.
11 Shit G C & Haldar R, *Int J Appl Math Mech*, 8 (2012a) 14.
12 Gireesha B J, Gorla R S R & Mahanthesh B, *J Nanofluids*, 4 (2015) 474.
13 Kumaran V & Ramanaih G, *Arch Mech*, 116 (1996) 229.
14 Vajravelu K, *Appl Math Comput*, 124 (2001) 281.
15 Cortell R, *Appl Math Comput*, 184 (2007) 864.
16 Bhargava R, Sharma S, Takhar H S, Bég O A & Bhargava P, *Non-linear Anal Model Control*, 12 (2007) 45.
17 Hayat T, Abbas Z & Javed T, *Phys Lett A*, 372 (2008) 637.
18 Awang S K & Hashim I, *Phys Lett A*, 372 (2008) 2258.
19 Hayat T, Hussain Q & Javed T, *Nonlinear Anal-Real World Appl*, 10 (2009) 966.
20 Ziabakhsh Z, Domairry G, Bararnia H & Babazadeh H, *J Taiwan Inst Chem Eng*, 41 (2010) 22.
21 Shahzad A A & Khan R M, *Chin Phys Lett*, 29 (2012) 084705.
22 Mukhopadhyay S, *Alexandria Eng J*, 52 (2013) 563.
23 Mahanthesh B, Gireesha B J, Gorla R S R, Abbasi F M & Shehzad S A, *J Magn Magn Mater*, 417 (2016) 189.
24 Rama P & Bhargava R, *Commun Nonlinear Sci Numer Simul*, 17 (2012) 212.
25 Rashidi M M, Freidoonimehr N, Hosseini A, Bég O A & Hung T K, *Meccanica*, 49 (2014) 469.
26 Hady F M, Ibrahim F S, Abael-Gaied S M & Eid M R, *Nanoscale Res Lett*, 229 (2012) 1.
27 Das K, *J Egypt Math Soc*, 23 (2015) 451.
28 Murshed F K, Roychowdhury I, Chattopadhyay A & Sandeep N, *Adv Phys Theor Appl*, 40 (2015) 43.
29 Khan J A, Mustafa M, Hayat T & Alsaedi A, *PloS One*, 9 (2014) 1.
30 Khan J A, Mustafa M, Hayat T & Alsaedi A, *Int J Heat Mass Transfer*, 86 (2015) 158.
31 Mahanthesh B, Gireesha B J & Gorla R S R, *J Nigerian Math Soc*, 35 (2016) 178.
32 Shit G C & Haldar R, *Therm Sci*, 15 (2011) 195.
33 Shit G C & Majee S, *J Appl Fluid Mech*, 7 (2014) 239.
34 Gireesha B J & Mahanthesh B, *Thermodynamics,* 2013 (2013) 1.
35 Gireesha B J, Mahanthesh B & Rashidi M M, *Int J Indust Math*, 7 (2015) 247.
36 Mahanthesh B, Gireesha B J & Gorla R S R, *Alexandria Eng J*, 55 (2016) 569.
37 Krupa Lakshmi K L, Gireesha B J, Gorla R S R & Mahanthesh B, *J Nigerian Math Soc*, 35 (2016) 66.
38 Ali M, Alim Md Abdul & Md Shah Alam, *Int J Adv Res Technol*, 3 (2014) 34.
39 Ashraf M B, Hayat T, Shehzad S A & Alsaedi A, *AIP Advances*, 5 (2015) 1.